Low energy cost for optimal speed and control of membrane fusion

Claire François-Martin, James E. Rothman, Frederic Pincet

Classification:

Major: Physical Sciences

Minor: Biophysics

TITLE

Low energy cost for optimal speed and control of membrane fusion

AUTHORS

Claire François-Martin[1], James E. Rothman[2*], Frederic Pincet[1,2*]

1. Laboratoire de Physique Statistique, Ecole Normale Supérieure, PSL Research University; Université Paris Diderot Sorbonne Paris Cité; Sorbonne Universités UPMC Univ Paris 06, CNRS; 24 rue Lhomond, 75005 Paris, France
2. Department of Cell Biology, Yale University School of Medicine, 333 Cedar Street, New Haven, CT 06520, United States
*Correspondence to: pincet@lps.ens.fr and james.rothman@yale.edu

KEYWORDS

Membrane fusion, activation energy, liposome, energy landscape.

ABSTRACT

Membrane fusion is the cell's delivery process, enabling its many compartments to receive cargo and machinery for cell growth and inter-cellular communication. The overall activation energy of the process must be large enough to prevent frequent and non-specific spontaneous fusion events, yet must be low enough to allow it to be overcome upon demand by specific fusion proteins (such as Soluble NSF Attachment Protein Receptors, SNAREs). Remarkably, to the best of our knowledge, the activation energy for spontaneous bilayer fusion has never been measured. Multiple models have been developed and refined to estimate the overall activation energy and its component parts, and they span a very broad range from 20 k_BT to 150 k_BT depending on the assumptions. In this study, using a bulk lipid mixing assay at various temperatures, we report that the activation energy of complete membrane fusion is at the lowest range of these theoretical values. Typical lipid vesicles were found to slowly and spontaneously fully fuse with activation energies of ~30 k_BT. Our data demonstrate that the merging of membranes is not nearly as energy-consuming as anticipated by many models, and is ideally positioned to minimize spontaneous fusion while enabling rapid, SNARE-dependent fusion upon demand.

SIGNIFICANCE STATEMENT

Membrane fusion is a key process for cell growth and inter-cellular communication. There are many models for fusion with widely divergent activation energies. Surprisingly, no comprehensive quantification of fusion was ever experimentally performed. Probably this is because of the difficulty of observing and quantifying rare spontaneous fusion events and equally the difficulty of establishing that such events are *bona fide* fusion events. Here, we find that the activation energy is lower by far than in most predictions. The biological importance of this low energy value is that it explains how cells can maintain traffic among distinct compartments without mixing them up, preventing spontaneous fusion but allowing specific delivery of cargo as soon as fusion-inducing proteins are in place.

\body

Living organisms and cells are composed of different compartments delimited by a membrane. These compartments have their own function and integrity but nevertheless need to communicate with one another. A common pathway by which exchanges can occur between them is membrane fusion, a crucial process leading to the opening of a fusion pore connecting two compartments and allowing their respective contents to mix or react(1, 2). The global effective activation energy of the process must be large enough to avoid frequent spontaneous membrane fusion events. Nevertheless, it must remain sufficiently low so that proteins like SNAREs (soluble N-ethylmaleimide–sensitive factor attachment protein receptor)(3-5) are able to overcome it and induce fusion. If multiple models(6-16) have been developed and refined to estimate this activation energy, there is still a lack of experimental data to provide its actual value and validate these models. Activation energies have been reported between intermediate states of the fusion process(17) or with non-phospholipid surfactants(18). They were obtained with non-spontaneous fusion triggered by an external source such as osmotic pressure or mechanical shear.

Here, by using a minimal membrane model system, we show that the activation energy of complete and spontaneous membrane fusion is in the lowest range of the predicted values. Lipid vesicles composed of POPC (1-palmitoyl-2-oleoyl-*sn*-glycero-3-phosphocholine) or DOPC (1,2-dioleoyl-*sn*-glycero-3-phosphocholine) were found to slowly and spontaneously fully fuse with respective activation energies of $26.4 \pm 1\ k_BT$ and $34.3 \pm 0.8\ k_BT$. Our data demonstrate that the merging of membranes is not as energy-consuming as anticipated in the early models.

While key aspects of the transition states remain unclear, lipid bilayer fusion likely involves intermediates(19) and is therefore kinetically complex. With this in mind, we take a more global view, in which kinetic complexity and molecular rearrangements are averaged to enable a simple experimental approach to measure activation energy by population analysis. Working in bulk with small phospholipid vesicles that undergo random Brownian motion provides an ideally controlled minimal system to monitor fusion on a large scale. Vesicles collide and, on very rare occasions these collisions are sufficiently energy-yielding to trigger fusion. When fusion is intentionally triggered by proteins like SNAREs or physico-chemical factors such as osmotic pressure, conditions are invariably chosen to minimize the rate of this spontaneous fusion so the fusion signal resulting from these rare spontaneous events is negligible.(3, 20) In principle, at high collision frequency, these fusion events can become numerous enough to be observable. Hence, to observe and quantify spontaneous fusion, we chose to use a classical bulk fusion assay with increased collision rate by working at high vesicle concentration with refined analysis.

Fusion among ~ 60 nm diameter phosphatidylcholine (PC) vesicles at 37 °C was monitored using a well-established lipid mixing assay(21) (Methods). Briefly, two sets of vesicles were mixed together. One set of vesicles contained two types of fluorescent lipids tagged with either NBD (7-nitro-2-1,3-benzoxadiazol-4-yl) or Rh (lissamine rhodamine B). These fluorescent lipids were present at concentrations at which NBD is largely quenched by Rh through FRET (*Förster resonance energy transfer*). The other set of vesicles were not fluorescent. When a fusion event occurs between a fluorescent vesicle and a non-fluorescent vesicle, the mixing of their lipids leads to dilution of the dyes in the resulting combined membrane. This dilution is associated with a decrease of FRET and can be

experimentally observed as an increase in NBD fluorescence which, when monitored in bulk, directly yields the number of fusion events per second, *i.e.* fusion speed.(3) To optimize the collision rate, vesicles were incubated at unusually high concentrations (18 mM PC). The results presented in Fig 1A show that lipid mixing was indeed readily observed, suggesting that detectable fusion-like events were occurring in the vesicle solution on experimental time-scales (~1 hr).

Before quantifying the energies involved, the remaining difficulty was to determine what these events actually correspond to: are they full fusion, intermediate fusion states, or merely lipid exchange without fusion? To discriminate among these possibilities, we monitored lipid mixing of the inner leaflets only. The fluorescent-lipid containing vesicles were first pre-incubated with dithionite (Supplementary Methods), which quenches NBD's fluorescence as it chemically reduces the NBD groups on the external leaflet only because dithionite does not cross lipid bilayers(22). Since the resulting vesicles only had fluorescent NBD in their inner leaflets (Fig. S1) any FRET changes resulting from incubation with the unlabeled vesicles could only be due to a dilution of their inner leaflet lipids, *i.e.* full fusion events, and not hemi-fusion (mixing of outer leaflets without inner leaflet fusion) or exchange of lipids between vesicles via their outer leaflets. Inner leaflet mixing was indeed observed at essentially the same rate as total lipid mixing (Fig. 1A), implying that the vast majority of the FRET signal was due to full fusion. To independently confirm this conclusion, we observed the samples by cryo-electron microscopy following incubation (60 minutes at 37 °C). Stable, extended hemi-fusion structures are readily observable by this method(23). However, we observed no such hemi-fusion diaphragms among the 4215 vesicles. Since FRET experiments show that ~2% of the vesicles have fused at the end of the experiment at 37°C (or 4% have hemifused), ~150 hemi-fusion diaphragms could have potentially been observed. This suggests that at least ~99% of the events led to full fusion (Fig. 1B and supplementary text). Taken together, the dithionite and cryo-EM results show that full vesicle fusion can result solely from spontaneous collisions in the course of Brownian motion and that, on the time-scale of our experiment, *i.e.* minutes, vesicles either remained intact or underwent complete fusion.

Thus, the process of spontaneous fusion among a large population of vesicles can be formulated as a two-state kinetic transition from two separate vesicles to a single vesicle because the lifespan of the intermediate states must be much shorter than the timescale of the experiment. This in turn establishes from a physical viewpoint that spontaneous fusion of vesicles represents a system to which Kramer's theory of reaction rates applies(24, 25). In the over-damped limit of this theory, the transition rate, which here is the speed of spontaneous fusion, follows a simple Arrhenius-like expression: $v=v_0\ exp(-E_a/k_BT)$, where k_B is the Boltzmann constant, v_0 is the frequency factor which depends on many parameters including the collision rate and the density of defects on the membrane, and E_a is an effective activation energy. The energy of the fusion process can thus be reduced to a single activation energy which corresponds to the height of the one energy barrier that must be overcome for full fusion to proceed, and would be crossed with the same probability as the actual, much more complex, energy landscape of the entire process. Since the Arrhenius law stipulates that the speed of spontaneous fusion increases with temperature in an E_a-dependent manner, we studied the fusion of POPC (1-16:0, 2-18:1 PC) and DOPC (di C18:0- PC) vesicles at temperatures, ranging from 27°C to 47°C (Fig. 2A) in order to determine their activation energies for fusion at 37°C, the physiological temperature. Since E_a and v_0 may vary with the temperature in a logarithmic way compared to $exp(-E_a/k_BT)$ (24-26), we chose a range of temperature that is small enough to remain close to 37°C and large enough to observe clear variations of the fusion speed.

Over this temperature range, the results showed that variations in the fusion speed are sufficiently large to accurately determine E_a at 37°C. The initial speeds of fusion were deduced from the initial slopes of the fusion curves (Supplementary Text). For both POPC and DOPC, the initial fusion speed varies with 1/T in an exponential manner, which *a posteriori* validates the Arrhenius-like dependence of the fusion speed (Fig. 2B). The activation energy values were determined through independent fits of the different experiments (9 for POPC and 4 for DOPC): 26.4 ± 1.0 k_BT for POPC and 34.3 ± 0.8 k_BT for DOPC at 37°C (Fig. 2C, error bars are standard error on the mean). To ensure that these values were not affected by the rate of collision of the liposomes we performed the same measurements at lower concentrations, 6 mM and 12 mM, without any change in the resulting activation energies.

For a more complex reaction pathway to result in the same overall probability of transition to the fused state as a pathway with a single activation barrier, the E_a deduced from the Arrhenius law in the simple two-state model must be larger than, or close to, any of the individual energy barriers that separate successive transient intermediate states in the more complex reaction process, as illustrated in Figure 3. Since most published models of the fusion process have focused on these proposed individual energy barriers, our results now make it possible to objectively evaluate the plausibility of these models. For both DOPC and POPC, we measured E_a close to 30 k_BT. Such a low value for the overall fusion process was never predicted but remains consistent with recently published coarse grained simulations(14, 16) in which there is no prior hypothesis concerning the fusion pathway, thereby allowing the predicted transition structures and activation energies to emerge directly. Our measured global E_a is indeed larger than or close to these. According to Smirnova *et al.*(14), 20 k_BT are required for stalk formation while Ryham *et al.*[16] evaluated activation energies of 31 k_BT (stalk) and 35 k_BT (fusion pore). Thus, these predictions are compatible with our experimental measurements and may closely reproduce the reality of the fusion process at a molecular scale. The previous theoretical studies predicted E_a much larger than 30 k_BT, ranging from 43 to 170 k_BT (10). Therefore, the assumptions underlying these models seem unlikely to hold.

An activation energy of ~30 k_BT can also be related to the short-range interactions between membranes that were characterized in the 1980s by Rand and Parsegian(27, 28). Using osmotic pressure, they compressed lamellar phases while measuring their interbilayer separation distance (d). They found that the pressure decreased exponentially with d for all phospholipids: $P(d)=P_0 \exp(-d/\lambda)$. This pressure results from the need to remove the bound water from the polar heads of the lipids as the distance shortens and/or from the entropic repulsion of the headgroups. The pre-factor P_0 and the decay (non-specific) length λ depended on the lipid composition but remained within the same range, 10^9 Pa and 0.15 nm respectively. Rand and Parsegian also observed that the lamellar phases were usually unstable when the distance was below ~1 nm, at which point an all-or-none transition to a non-lamellar phase occurred, which these authors suggested resembles the transition from unfused to fused states for vesicles. With these values, the surface energy required for the transition is of the order of 1 mJ/m^2 (Supplementary Text). 30 k_BT would be distributed over an area of a ~600 nm^2 (Supplementary Text) and therefore involving only ~1000 phospholipids (which occupy about 0.7 nm^2 surface each(27)). Though the analogy between the two systems is clearly imperfect because there are many subtle uncontrolled aspects such as kinetics and membrane tension, this value would correspond to the cooperative unit of surface on which the future fusion pore will develop and is compatible. This size seems reasonable since it is compatible with the radius of the initial fusion pore is thought to be close to one nanometer(29).

Finally, 30 k_BT is an ideal value to enable facile membrane fusion as directed on demand in living cells: it will not happen spontaneously between bare membranes, yet as soon as specific fusion machinery is in place, it will be easily triggered. Fusion between two given membranes is a stochastic event that occurs on average after a time $\tau = \tau_0 \exp(E_a/k_BT)$. Depending on the context (membranes, geometry), the pre-factor is between 10^{-10} and 10^{-6}s.(24, 30) For E_a=30 k_BT, spontaneous fusion will occur between closely apposed phospholipid membranes after 15 minutes to 100 days (Supplementary Text). Therefore, at the relevant biological scale at which specific fusion occurs (seconds to minutes) it will very seldom happen. However, a single SNAREpin in place between the membranes will significantly lower the activation energy barrier and allow fusion to proceed on the biological timescale. For example, even assuming that the assembly of the linker domain in the C-terminal region of the cytosolic portion is the sole energy supplier for bilayer fusion, the reduction in activation energy will be ~10 k_BT (31), so E_a now becomes ~20 k_BT which lowers the average time for fusion to the range 50 ms - 5 min, depending on the pre-factor. This explains why a single SNARE complex can mediate many fusion processes in isolated systems.(32, 33) When more SNARE complexes are involved, the activation energy is correspondingly reduced and the time required becomes exponentially shorter. This increase in the number of SNARE complexes is necessary in specific cases such as neurotransmission in which synaptic vesicles must fuse with the presynaptic plasma membrane in less than a millisecond(34). This drastic time-scale change shows that our measured value for activation energy of ~30 k_BT is an elegant balance that nature has made, preventing spontaneous fusion, thus allowing the cell to maintain distinct membrane-bound compartments, yet quickly overcoming this barrier when SNARE and other fusion-inducing proteins are put in place, thus enabling specific traffic among these compartments.

Supporting information

Supporting Text, Methods and Figures S1-S2.

Author contributions

J.E.R. and F.P. initiated the project. C.F.-M. and F.P. designed the experiments. C.F.-M. performed the experiments. All authors analyzed the data and prepared, reviewed and approved the manuscript.

Acknowledgments

C.F.-M. thanks the Direction Générale de l'Armement (DGA) for their financial support. This work was supported by Agence Nationale de la Recherche (ANR) ANR-14-1CHN-0022-01 grant to J.E.R.. The authors are grateful to Dr. Abdou-Rachid Thiam for fruitful discussions and Dr. Steve Donaldson for reading and commenting the manuscript. The authors thank Aurélie Di Cicco for the Cryo-EM experiments which were supported by the French National Research Agency through the "Investments for the Future" program (France-BioImaging, ANR-10-INSB-04) and were performed at the PICT-IBiSA Institut Curie, Paris, member of the France-BioImaging national research infrastructure.

References

1. Jahn R, Lang T, & Sudhof TC (2003) Membrane fusion. *Cell* 112(4):519-533.
2. Rothman JE (2014) The principle of membrane fusion in the cell (Nobel lecture). *Angew Chem Int Ed Engl* 53(47):12676-12694.
3. Weber T*, et al.* (1998) SNAREpins: minimal machinery for membrane fusion. *Cell* 92(6):759-772.

4. Jahn R & Scheller RH (2006) SNAREs--engines for membrane fusion. *Nat Rev Mol Cell Biol* 7(9):631-643.
5. Wickner W & Schekman R (2008) Membrane fusion. *Nature structural & molecular biology* 15(7):658-664.
6. Kozlov MM, Leikin SL, Chernomordik LV, Markin VS, & Chizmadzhev YA (1989) Stalk mechanism of vesicle fusion. Intermixing of aqueous contents. *Eur Biophys J* 17(3):121-129.
7. Siegel DP (1993) Energetics of intermediates in membrane fusion: comparison of stalk and inverted micellar intermediate mechanisms. *Biophys J* 65(5):2124-2140.
8. Kuzmin PI, Zimmerberg J, Chizmadzhev YA, & Cohen FS (2001) A quantitative model for membrane fusion based on low-energy intermediates. *Proc Natl Acad Sci U S A* 98(13):7235-7240.
9. Markin VS & Albanesi JP (2002) Membrane fusion: stalk model revisited. *Biophys J* 82(2):693-712.
10. Kozlovsky Y & Kozlov MM (2002) Stalk model of membrane fusion: solution of energy crisis. *Biophys J* 82(2):882-895.
11. Kozlovsky Y, Chernomordik LV, & Kozlov MM (2002) Lipid intermediates in membrane fusion: formation, structure, and decay of hemifusion diaphragm. *Biophys J* 83(5):2634-2651.
12. May S (2002) Structure and energy of fusion stalks: the role of membrane edges. *Biophys J* 83(6):2969-2980.
13. Kozlovsky Y, Efrat A, Siegel DP, & Kozlov MM (2004) Stalk phase formation: effects of dehydration and saddle splay modulus. *Biophys J* 87(4):2508-2521.
14. Smirnova YG, Marrink SJ, Lipowsky R, & Knecht V (2010) Solvent-exposed tails as prestalk transition states for membrane fusion at low hydration. *J Am Chem Soc* 132(19):6710-6718.
15. Kawamoto S & Shinoda W (2014) Free energy analysis along the stalk mechanism of membrane fusion. *Soft Matter* 10(17):3048-3054.
16. Ryham RJ, Klotz TS, Yao L, & Cohen FS (2016) Calculating Transition Energy Barriers and Characterizing Activation States for Steps of Fusion. *Biophys J* 110(5):1110-1124.
17. Lee J & Lentz BR (1998) Secretory and viral fusion may share mechanistic events with fusion between curved lipid bilayers. *Proc Natl Acad Sci U S A* 95(16):9274-9279.
18. Porcar L, Hamilton WA, Butler PD, & Warr GG (2004) Topological relaxation of a shear-induced lamellar phase to sponge equilibrium and the energetics of membrane fusion. *Phys Rev Lett* 93(19):198301.
19. Chernomordik LV & Kozlov MM (2008) Mechanics of membrane fusion. *Nature structural & molecular biology* 15(7):675-683.
20. Meyenberg K, Lygina AS, van den Bogaart G, Jahn R, & Diederichsen U (2011) SNARE derived peptide mimic inducing membrane fusion. *Chemical communications* 47(33):9405-9407.
21. Struck DK, Hoekstra D, & Pagano RE (1981) Use of resonance energy transfer to monitor membrane fusion. *Biochemistry* 20(14):4093-4099.
22. McIntyre JC & Sleight RG (1991) Fluorescence assay for phospholipid membrane asymmetry. *Biochemistry* 30(51):11819-11827.
23. Hernandez JM*, et al.* (2012) Membrane fusion intermediates via directional and full assembly of the SNARE complex. *Science (New York, N.Y* 336(6088):1581-1584.
24. Kramers HA (1940) Brownian motion in a field of force and the diffusion model of chemical reactions. *Physica (Utrecht)* 7:284-304.
25. Hanggi P, Talkner P, & Borkovec M (1990) Reaction-Rate Theory - 50 Years after Kramers. *Reviews of Modern Physics* 62(2):251-341.
26. Evans E & Smith BA (2011) Kinetics of Hole Nucleation in Biomembrane Rupture. *New J Phys* 13.

27. Rand RP & Parsegian VA (1989) Hydration Forces between Phospholipid-Bilayers. *Biochimica Et Biophysica Acta* 988(3):351-376.
28. Rand RP & Parsegian VA (1986) Mimicry and mechanism in phospholipid models of membrane fusion. *Annu Rev Physiol* 48:201-212.
29. Breckenridge LJ & Almers W (1987) Currents through the fusion pore that forms during exocytosis of a secretory vesicle. *Nature* 328(6133):814-817.
30. Evans E (2001) Probing the relation between force--lifetime--and chemistry in single molecular bonds. *Annu Rev Biophys Biomol Struct* 30:105-128.
31. Zorman S*, et al.* (2014) Common intermediates and kinetics, but different energetics, in the assembly of SNARE proteins. *eLife* 3:e03348.
32. Shi L*, et al.* (2012) SNARE proteins: one to fuse and three to keep the nascent fusion pore open. *Science (New York, N.Y* 335(6074):1355-1359.
33. van den Bogaart G*, et al.* (2010) One SNARE complex is sufficient for membrane fusion. *Nature structural & molecular biology* 17(3):358-364.
34. Sudhof TC (2004) The synaptic vesicle cycle. *Annual review of neuroscience* 27:509-547.
35. Evans E (1991) Entropy-Driven Tension in Vesicle Membranes and Unbinding of Adherent Vesicles. *Langmuir* 7(9):1900-1908.
36. Parlati F*, et al.* (1999) Rapid and efficient fusion of phospholipid vesicles by the alpha-helical core of a SNARE complex in the absence of an N-terminal regulatory domain. *Proceedings of the National Academy of Sciences of the United States of America* 96(22):12565-12570.

FIGURE LEGENDS

Figure 1: Full fusion is achieved spontaneously in a suspension of POPC vesicles and intermediate states are transient. (A) In the classical lipid mixing assay (empty diamonds), where the fusion of fluorescent and non-fluorescent vesicles is monitored (See text and Method), the increase of the fluorescence intensity of NBD shows that lipid mixing takes place and, hence, suggests that fusion-like events occur. The dithionite assay (filled triangles), monitoring the fusion of fluorescent vesicles pre-treated with dithionite and non-fluorescent vesicles, shows that mixing of lipids coming from the inner leaflets occurs. The dithionite pre-treatment of the fluorescent vesicles removes NBD (black filled circles in the schematic vesicles) from the outer leaflets of vesicles. Rh is present on both leaflets and is not represented on the schematic vesicles. This demonstrates that full-fusion events occur. The perfect superimposition of both curves (diamonds and triangles) proves that neither hemi-fusion nor lipid exchange through the solvent significantly occur, and that the large majority of the events leading to lipid mixing are full fusion. (B) Representative cryo-electron micrograph. The enlarged pairs of vesicles represent two of the rare cases in which two vesicles are in close apposition. The presence of vesicles inside the largest one (which was observed in the minority of the vesicles) only lowered the effective concentration of vesicles. Since we always used the same pool of vesicles for all temperatures, this does not impact the results. Scale bar: 500nm. No hemi-fusion diaphragm was observed among 4215 vesicles which would correspond to ~150 fusion events (See SI).

Figure 2: Estimate of the activation energy of POPC and DOPC vesicles fusion. (A) Fusion assays are performed at different temperatures (27°C – 47°C). The averages of six independent experiments are represented. The initial time (t=0) is the time where the temperature was stabilized. The speed of fusion increases with temperature. Error bars are standard errors on the mean. (B) Initial spontaneous fusion speeds are represented vs. the temperature (average of nine independent experiments for POPC and four for DOPC,

error bars being standard deviations), and fitted by exponentials. Speeds of fusion were determined thanks to the initial slope of the curve representing the percentage of fused vesicles per minute (Supplementary text). (C) The exponential fits allow the determination of the activation energies for both reactions, here fusion. Independent fits were also performed for the different experiments, hence allowing the estimation of the error on the measurement (standard error on the mean): 26.4 ± 1 k_BT for POPC, and 34.3 ± 0.8 k_BT for DOPC.

Figure 3: Lipid bilayer fusion's energy landscapes of decreasing complexity. (left) Schematics of a typical model of the complete energy landscape of the fusion pathway of lipid bilayers. It exhibits three energy barriers: one for the stalk formation, one for the expansion of the hemi-fusion diaphragm and one for the opening of the fusion pore. (right) Schematics of an effective energy landscape of the fusion pathway. The three former energy barriers can be represented by one effective energy barrier, of which the height corresponds to the effective activation energy (E_a of the overall process of fusion. The speed of fusion then follows Arrhenius law: $v=v_0\ exp(-E_a/k_BT)$ and is the same for the three-barriers and one-barrier fusion pathways.

Figure 1

(A)

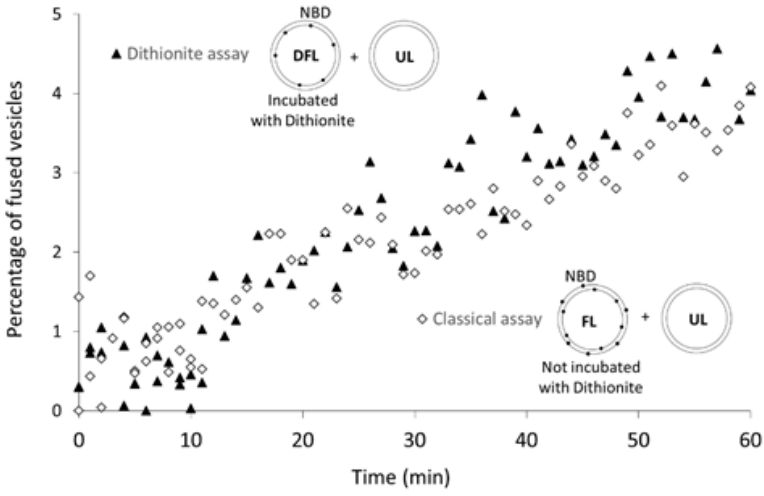
Percentage of fused vesicles
Time (min)
0
10
20
30
40
50
60
1
2
3
4
5
Dithionite assay
NBD
DFL
UL
Incubated
with Dithionite
Classical assay
NBD
FL
UL
Not incubated
with Dithionite

(B)

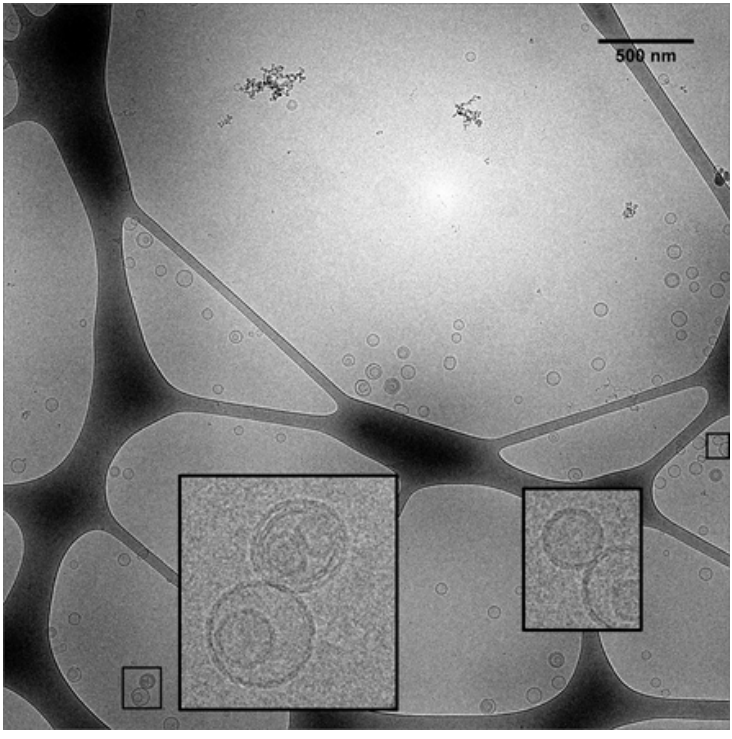
500 nm

Figure 2

(A)

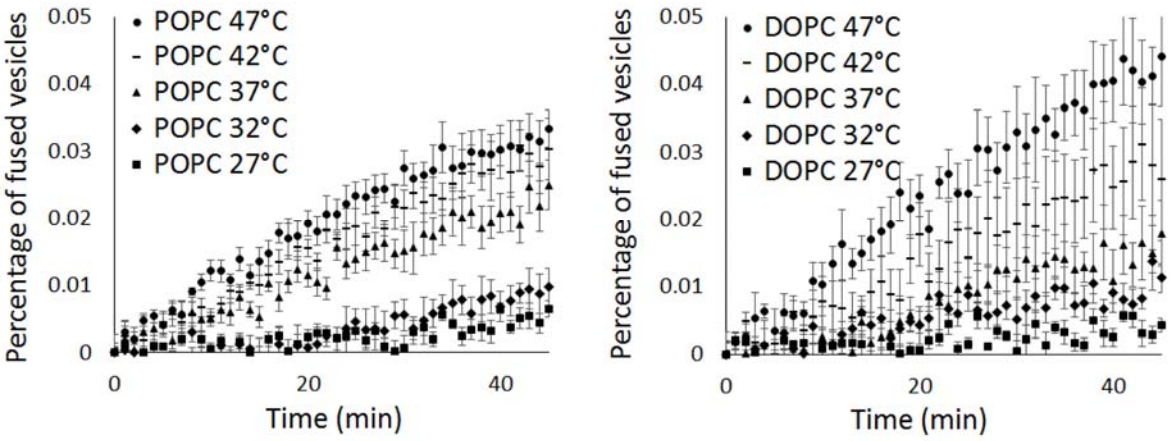

(B)

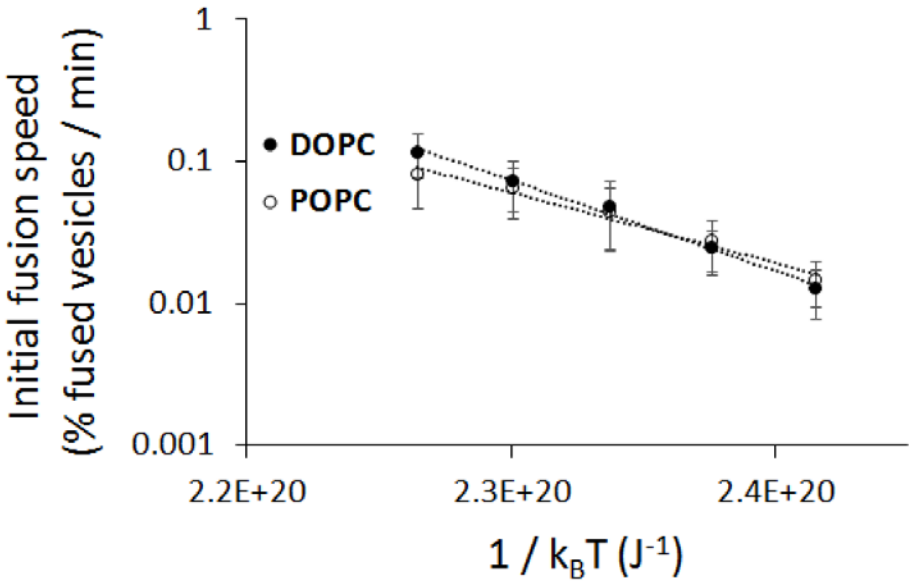

(C)

Lipid composition	Fit (average data)	E_a (average data)	E_a
POPC	$y = 1.36E+08e^{-1.14E-19x}$	26.6 k_BT	26.4 ± 1.0 k_BT
DOPC	$y = 3,27E+11e^{-1,47E-19x}$	34.3 k_BT	34.3 ± 0.8 k_BT

Figure 3

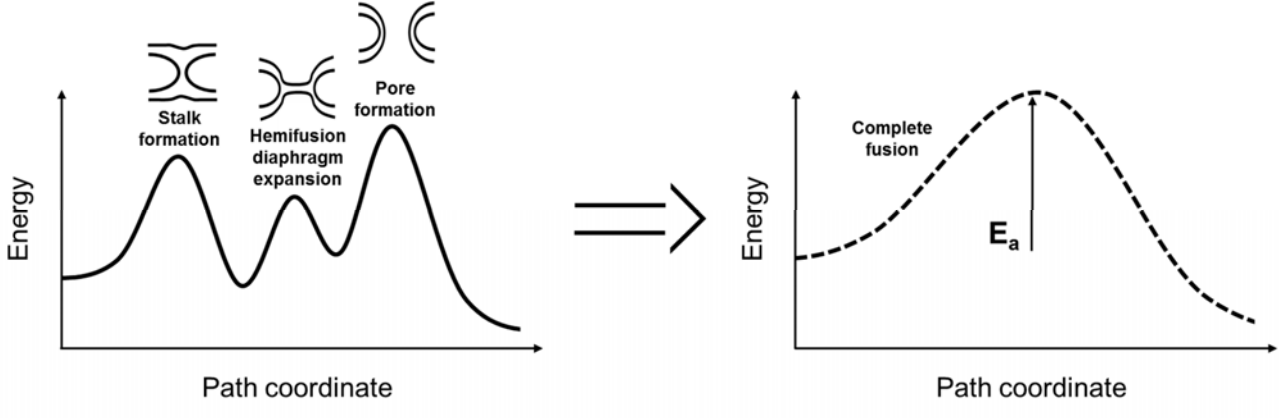
Stalk formation
Hemifusion diaphragm expansion
Pore formation
Energy
Path coordinate
Complete fusion
E_a
Energy
Path coordinate

Low energy cost for optimal speed and control of membrane fusion

Claire François-Martin, James E. Rothman, Frederic Pincet

Supplementary information

SUPPORTING TEXT

Estimate of the fraction of vesicles in hemifused state

After 60 minutes, ~3% of the vesicles underwent a full fusion-like event (Fig 1A) or equivalently ~6% underwent hemifusion. This percentage would represent ~150 (resp. ~300) vesicles that fused (resp. hemi-fused). Since we did not observe any hemifused vesicle among a total of 4215 (from 67 electron micrographs), the fraction of vesicles that underwent a fusion-like event and that are trapped in the extended-hemifusioned state is lower than 1%.

Surface energy for the transition from lamellar to non-bilayer phase

Using osmotic pressure, Rand and Parsegian(27) compressed lamellar phases while measuring their interbilayer separation distance (d). They found that the pressure decreased exponentially with d for all phospholipids: $P(d)=P_0 \exp(-d/\lambda)$. They also observed that the lamellar phases were usually unstable when the distance was below d_{min}~1 nm, at which point an all-or-none transition to a non-lamellar phase occurred. To reach this intermembrane distance, it is necessary to mechanically work against the intermembrane pressure. Physically, this leads to a dehydration of the membranes.

Thus, the surface energy for the transition is represented by the work of the interbilayer pressure when bringing the membrane from a large separation to the transition separation distance, i.e.:

$$E_{surf} = \int_{d_{min}}^{+\infty} P_0 \exp\left(-\frac{d}{\lambda}\right) \mathrm{d}d$$

With P_0=10^9 Pa and λ=0.15 nm, $E_{surf} \sim P_0 \lambda \exp\left(-\frac{d_{min}}{\lambda}\right)$ =0.2 mJ.m^{-2}.

Hence, the activation energy we measure, Ea, corresponds to an area: E_a/E_{surf}= 30 k_BT/0.2 mJ/m^2=600 nm^2. This size of this area is large enough to accomodate the initial fusion pore: radius ~1nm to which the thickness of two bilayers must be added, *i.e* a total diameter equal to ~12 nm corresponding to ~100 nm^2.

Fusion and close apposition of membranes

Membranes that are far apart will never fuse. Hence, to spontaneously fuse, membranes need to come in close vicinity. This is what happens during collisions in bulk. Since collision times are short, the likely-hood of fusion per collision is extremely low. However, in cells, membranes are often kept in contact by specific factors that tether them together. Pure phospholipid membranes also spontaneously adhere through van der Waals interactions at equilibrium distances of the order of a few nm(35). When the membranes are thereby held in proximity to one another, fluctuations make them constantly collide and, on average, fusion will occur after a time $\tau=\tau_0 \exp(E_a/k_BT)$. The pre-factor includes the specific features of each system, including the intermembrane distance.

SUPPORTING METHODS

Vesicle preparation

vesicles were prepared by drying the lipids (Avanti Polar Lipids), which were dissolved in chloroform, under nitrogen in a glass tube, submitting them to vacuum for more than two hours, and finally re-suspending them in a buffer solution (25mM HEPES, 100mM KCl, pH=7.4) to have a total lipid concentration of 18 mM. The solution was then frozen and thawed five times before being extruded 21 times through 50nm polycarbonate filters (Avanti Polar Lipids). The final diameter of the vesicles was 63 ± 16 nm (Fig. S2). Vesicles were conserved overnight at 4°C under argon for stabilization of the membranes prior to experiment. The non-fluorescent vesicles only contained 1,2-dioleoyl-sn-glycero-3-phosphocholine (DOPC) or 1-palmitoyl-2-oleoyl-*sn*-glycero-3-phosphocholine (POPC). The fluorescent vesicles contained DOPC (or POPC), 1,2-dioleoyl-*sn*-glycero-3-phosphoethanolamine-N-(lissamine rhodamine B sulfonyl) (Rh-PE) and 1,2-dioleoyl-*sn*-glycero-3-phosphoethanolamine-N-(7-nitro-2-1,3-benzoxadiazol-4-yl) (NBD-PE) in the molar ratio of 97:1.5:1.5.

Total lipid mixing fluorescence assay

To monitor the lipid mixing occurring between vesicles during fusion, fluorescent and non-fluorescent vesicles were mixed together at a 1:7 ratio to reach a final volume of 56 µL. The 1:7 ratio was chosen to optimize the signal to noise ratio of the "fusion signal". For small ratios, the total fluorescent signal of the sample is very low (small number of fluorescently tagged vesicles) so the signal to noise ratio also is. For large ratios, the total fluorescent signal is high but the probability of a given fluorescent vesicle to encounter, thus to fuse, with a non fluorescent one is low. Hence, a larger fraction of the fusion events do not go along with a fluorescence dequenching and the signal to noise ratio is low. A control experiment was performed in parallel by replacing non-fluorescent vesicles by the same volume of buffer.

The fluorescence was read from the bottom, at 538 nm for an excitation wavelength of 460 nm in a plate reader (SpectraMax M5e, Molecular Devices), with a transparent 96-well plate.

The maximum fluorescence intensity (MFI) was obtained by adding 50µL of Triton 4% (v/v). In presence of Triton above its critical micellar concentration, the lipids initially present in liposomes are solubilized in detergent micelles. Provided that enough detergent is added (in order to have enough micelles to have only ~1 fluorescent lipid per micelle), FRET is no longer possible between NBD and Rho. NBD thus presents its maximal fluorescence intensity (MFI). To be sure that enough Triton was added, an extra 50uL of Triton 4% was added to the sample, without a significant change in the MFI.

The experiments were carried at different temperatures between 27°C and 47°C.

Inner leaflet lipid mixing fluorescence assay

For the inner leaflet lipid mixing assay, 50µL of fluorescent vesicles at 18mM lipids were pre-treated at 37°C with 1µL of 1M solution of sodium dithionite (71699, Sigma Aldrich), to form a population of vesicles containing fluorescent NBD solely on the inner leaflet. As expected, after disappearance of the fluorescence from the outer leaflet, the NBD intensity was divided by two (Fig. S1). The end of the protocol is the same as for the total lipid mixing assay except that fluorescent vesicles were replaced by dithionite pre-treated fluorescent vesicles.

Data analysis

One of the difficulty of our approach was to accurately analyze the raw data to obtain the actual fusion speed. Theoretically, the MFI should correspond to the fluorescence intensity of NBD at infinite dilution (no FRET). Experimentally, the dilution is achieved by solubilizing the liposomes with detergent. Since the

quantum yield of NBD is not the same in the presence and absence of detergent and, moreover, this difference is sensitive to temperature, the MFI values were all corrected for the temperature effect. To determine these corrections, we prepared vesicles containing sufficiently low fractions of NBD and Rho (0.001%) in liposomes for no FRET to be possible. Adding detergent hence did not increase the signal since no further dequenching took place. Due to the changed environment, the signal actually decreased and the relative decrease was not the same at different temperatures. This allowed to determine the correction factors needed to be applied to the MFI values in order to obtain the real maximal fluorescence (only related to the number of fluorescent molecules, and not to temperature). They are 1.71 ± 0.03 at 27°C, 1.73 ± 0.03 at 32°C, 1.79 ± 0.03 at 37°C, 1.80 ± 0.01 at 42°C and 2.01 ± 0.02 at 47°C. One can see that the effect of temperature is significant and not correcting the MFI's may alter the value of Ea.
Then the control curve was subtracted from the sample curve and normalized by the corrected MFI value to make different experiments comparable.
Fluorescence signals where then converted to fusion extents (completed cycles of fusion), as presented in Parlati *et al.*(36). This was done by relying on a calibration curve linking the dequenching to different dilutions (see Parlati et al.). This type of curve can be obtained by measuring the fluorescence of samples presenting various known and controlled fractions of fluorescent lipids - mimicking the result from different dilutions. Because the vast majority of events are full fusion events, these completed cycle of fusion can be directly converted to the percentage of vesicles initially loaded in the well that underwent fusion (Fig. 1A and 2A).
The initial speed of fusion, in cycles of fusion per minute is then represented as the percentage of initially loaded vesicles that fuse per minute and is directly obtained as the slope of the final curve at t=0.

Electron microscopy
Vesicles were incubated at 37°C for at least 60 minutes. Other vesicles of the same batch where also kept at 4°C as control. The samples where then diluted to a lipid concentration of 3mM. Images were recorded under low-dose conditions with a FEI Tecnai20 laB6 electron microscope operating at 200 kV with a F416 CMOS camera (TVIPS, GmgH) 4096 pixel x 4096 pixel. The intended underfocus was set to -2 to -3 µm. Images of both conditions were collected at a nominal magnification of 11,500 and zoom-ins (magnification of 29,000) were performed when two vesicles where apposed, in order to see if they were hemifused. The size distribution of the vesicles is provided in Fig S2.

Supplementary figures captions

Figure S1: Dithionite incubation destroys the NBD of the outer leaflet only. Sodium dithionite at a concentration of 20mM (filled markers) or buffer (empty markers) was added after 7 minutes (black arrow) at 37°C to a solution of vesicles containing 1.5% of NBD-PE and 1.5% of Rh-PE on both leaflets. The two-fold decrease of the signal after the addition of dithionite shows that half of the NBD florescence disappeared, which is consistent with a complete quenching of the NBD from the sole outer leaflet. Since the fluorescence signal after dithionite remains stable over 30 minutes, there is no significant translocation of lipid between leaflets during the time frame of our experiment.

Figure S2: Size histogram of the POPC vesicle after overnight incubation at 4°C. The sizes have been determined by the measurement plugin of Image J of 6 micrographs (total 175 vesicles). We obtained a size of 63 ± 16 nm, error being the standard deviation. This distribution ranges between 30 and 100 nm in diameter which suggests that curvature effect may impact our measurements. Hence, it is

critical to ensure the fusion reaction we observe is not only due to a sub-population of the vesicles with specific diameters. This can be achieved by analyzing the slope variation in the fusion experiment. On average, we found that the slope decreases by ~10% of the initial slope (at t=0) after ~5% of the vesicles have fused (close to the end of the experiment in the fastest cases). The slope is proportional to the number of fluorescent vesicles accessible for fusion. Hence, a 10% decrease of the slope after 5% of the vesicles have fused means that 50% are involved in the fusion process. Even though these percentages are not precise because the slope variation is difficult to accurately determine, they mean that a significant fraction (tens of percent) of the vesicles are involved in the fusion process. This result shows that the fusion potent-vesicles cannot only correspond to a tiny sub-population. Thus, it can be considered here that the measured activation energy is actually that of vesicles having 60 nm diameter.

Because of the low percentage of fused vesicles (less than 5%, see caption of Fig. 1B), no significant change in the size distribution can be observed at the end of the experiment.

Figure S1

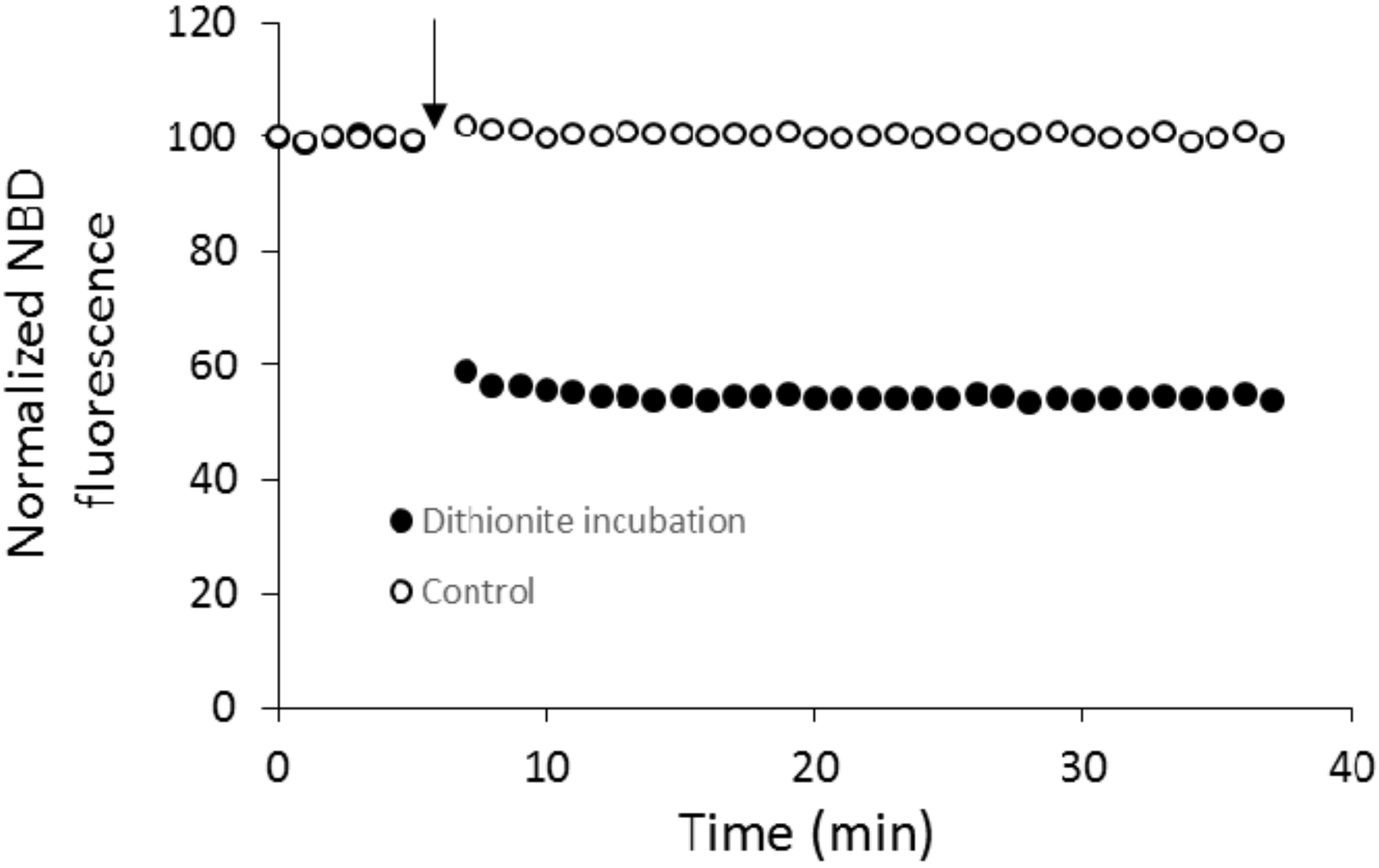
Normalized NBD fluorescence
120
100
80
60
40
20
0
0
10
20
30
40
Time (min)
Dithionite incubation
Control

Figure S2

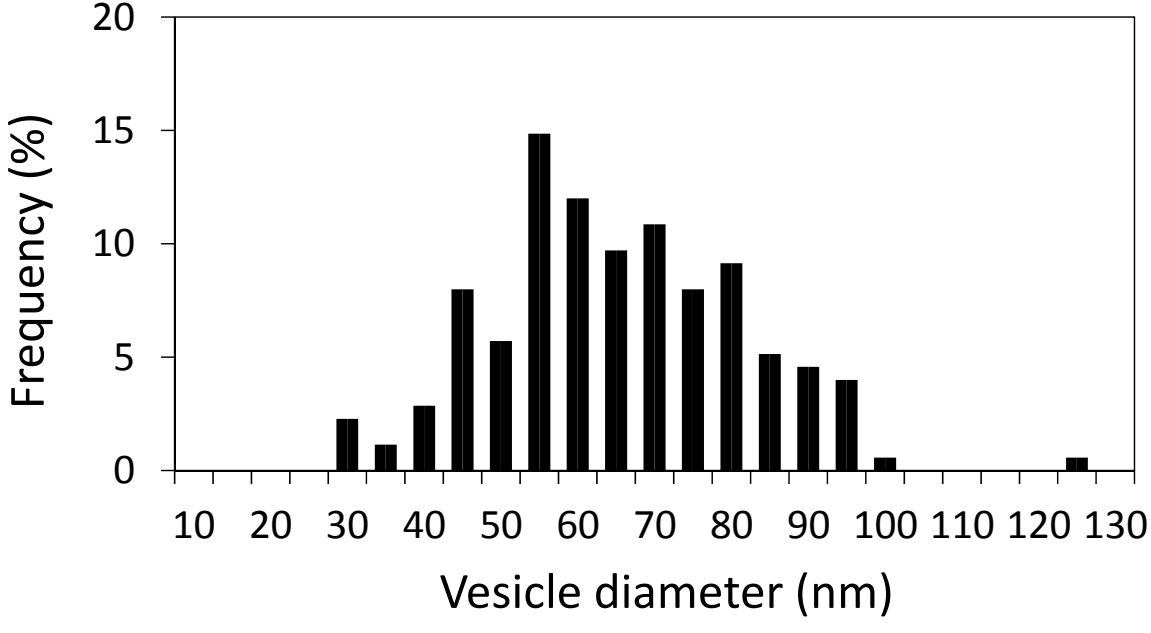
20
15
10
5
0
Frequency (%)
10 20 30 40 50 60 70 80 90 100 110 120 130
Vesicle diameter (nm)